A distal pocket Leu residue inhibits the binding of O_2 and NO at the distal site of cytochrome *c′*

Elizabeth M. Garton[†], David A. Pixton[†], Christine A. Petersen[†], Robert R. Eady[‡], S. Samar Hasnain[‡], and Colin R. Andrew[†*].

[†]Department of Chemistry and Biochemistry, Eastern Oregon University, La Grande, OR 97850, [‡] Molecular Biophysics Group, Faculty of Health and Life Sciences, Institute of Integrative Biology, University of Liverpool, Liverpool, L69 7ZB, UK.

SUPPLEMENTARY INFORMATION

Materials and Methods

Preparation of protein samples. Samples of AXCP were prepared as previously described.[1,2] Ferrous, oxy and nitrosyl complexes of L16A were prepared by first oxidizing the as-isolated form of the protein to the ferric state by reaction with a 2000-fold excess of 1 M ferricyanide solution at room temperature for 10 min. Excess ferricyanide was removed using a P6-DG desalting column. Ferrous L16A was generated inside an anaerobic glove box by reduction of the ferric protein with a ten-fold excess of 2-mM sodium dithionite solution. Excess reductant was removed using either a P6-DG desalting column or a minispin desalting column (Zeba filter, Pierce). Oxy and nitrosyl complexes of L16A AXCP were prepared by reaction of ferrous protein with buffer solution containing dissolved O_2 and NO, respectively.

RR spectroscopy. Protein samples for RR measurements were diluted to approximately 100 μM (in heme) using pH 7.0 buffer (50 mM MOPS, 0.1 M NaCl). The oxy complex of L16A was generated from ferrous protein by the introduction of either $^{16}O_2$ or $^{18}O_2$ gas into the headspace of a septum-sealed capillary tube using a gas-tight Hamilton syringe. The identity of RR samples was verified by UV-vis spectroscopy before and after exposure to the laser beam using a modified Cary 50 spectrophotometer. Resonance Raman (RR) spectra were recorded on a custom McPherson 2061/207 spectrograph (set to 0.67 m) equipped with a Princeton Instruments liquid N_2-cooled (LN-1100PB) CCD detector. Excitation wavelengths were provided by a Kr ion laser (413 nm), and a He-Cd laser (442 nm) and Rayleigh scattering was attenuated using Kaiser supernotch filters. RR spectra were collected at room temperature in a 90º-scattering geometry for periods of 5–10 minutes using laser powers of 5 – 10 mW measured at the sample. Frequencies were calibrated relative to aspirin and indene as standards, and are accurate to ±1 cm^{-1}.

Kinetic measurements and absorbance spectra. Kinetic measurements were conducted at 25.0 °C in pH 8.9 buffer containing 50 mM CHES and 0.1 M NaCl (to match previous reaction conditions for native AXCP) using an Applied Photophysics SX.18MV-R stopped-flow spectrophotometer (dead time ~1 ms) housed within an anaerobic glove box (Coy Laboratory Products Inc.). Rate constants for O_2 binding were determined by rapidly mixing a solution of ferrous L16A (~4 μM heme) with an equal volume of buffer containing dissolved O_2, and monitoring the formation of the oxy complex at 416 nm using a photomultiplier detector. Solutions of O_2 were prepared by equilibrating an O_2/N_2 gas mixture with buffer at 25.0 °C, assuming the concentration of 1 atm aqueous O_2 to be 1.3 mM. Concentrations of dissolved O_2 (26 – 104 μM after mixing) were maintained in at least 10-fold excess over the heme binding sites to ensure pseudo-first order conditions. Values of pseudo-first order rate constants, k_{obs}, were determined from single exponential fits of time courses, and are the average of 3–5 separate kinetic runs. The bimolecular rate constant for O_2 binding (k_{on}) was determined from the slope of plot of k_{obs} versus O_2 concentration. Rate constants for NO binding were obtained using a similar approach to that described above for O_2. In this case, concentrations of dissolved NO (42 – 136 μM after mixing) were prepared by equilibrating an NO/N_2 gas mixture with buffer at 25.0 °C, assuming the concentration of 1 atm aqueous NO to be 1.9 mM.

The O_2 off-rate constant, $k_{off}(O_2)$ for L16A was determined by reacting the oxy complex with a solution of sodium dithionite (5 – 400 mM) as O_2 scavenger.[3] The reaction mixture also contained ~0.5 mM CO which rapidly binds to pentacoordinate ferrous heme of the L16A variant, thereby trapping and stabilizing the heme upon O_2 release. Under these conditions, O_2 release was monitored via the rate of L16A CO complex formation (absorption increase at 418 nm) with the rate-determining step being O_2 release from heme. This was confirmed by the observation that the

rate was insensitive to variations in dithionite concentration (5 - 400 mM) as well as the presence or absence of CO. Using an approach similar to that described above for determining $k_{off}(O_2)$, the release of NO from L16A was studied by reacting the nitrosyl complex with a solution of 28-56 mM sodium dithionite (as NO scavenger) in the presence of ~0.5 mM CO. Under these conditions, the release of NO is apparent from conversion of the 6c heme-NO complex to that of the 6c heme-CO complex (Figure S9a). The release of NO from L16A AXCP is extremely slow, with only ~ 20% of the expected absorbance change occurring after 19 days (Figure S9a). An exponential fit of the 417-nm absorbance time course (with the final absorbance constrained to the predicted value for the pure 6c-CO end product) yields k_{off} ~ 0.013 day^{-1} (~ 2×10^{-7} s^{-1}). Kinetics measurements over longer time periods were prevented due to reagent and protein instability.

The reaction of native AXCP with O_2 at pH 8.9 was analyzed by the stopped flow technique. Ferrous native AXCP (prepared in a similar manner to that described above for the L16A variant) was mixed with solutions containing air-saturated buffer in a 1:1 ratio. Time-resolved absorbance spectra (300 – 700 nm) were recorded using a photodiode array detector over a period of 15 min. Global analysis of kinetic data was performed using the Pro Kineticist software package. Ferrous protein converted to the ferric form in a monophasic reaction without any detectable oxy complex (Figure S6) with an observed rate constant, $k_{ox} = 4 (\pm 1) \times 10^{-3}$ s^{-1}.

Figure S1. Absorbance spectra of Fe^{2+} and oxy L16A AXCP (~2 μM), together with the 416-nm time trace for oxy formation (26 μM O_2).

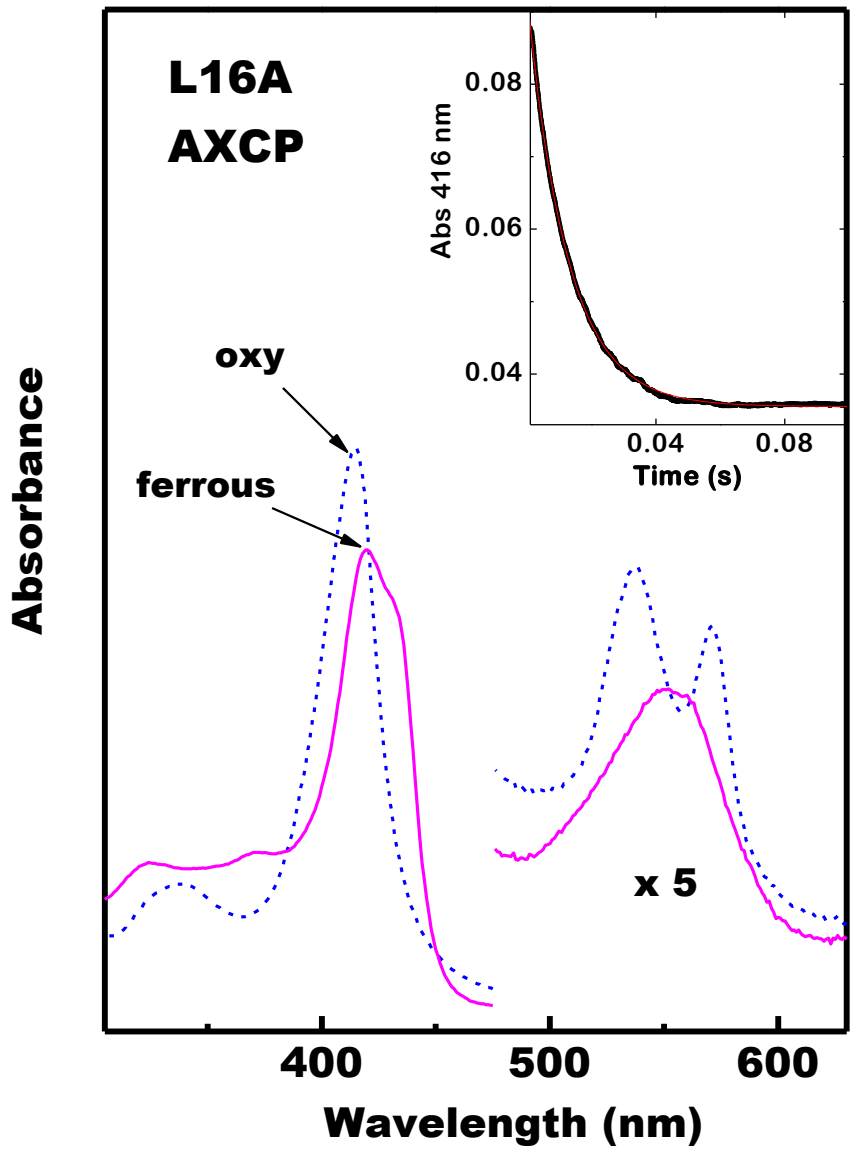

Figure S2. High-frequency RR spectrum of 6c-O_2 L16A AXCP complex at room temperature.

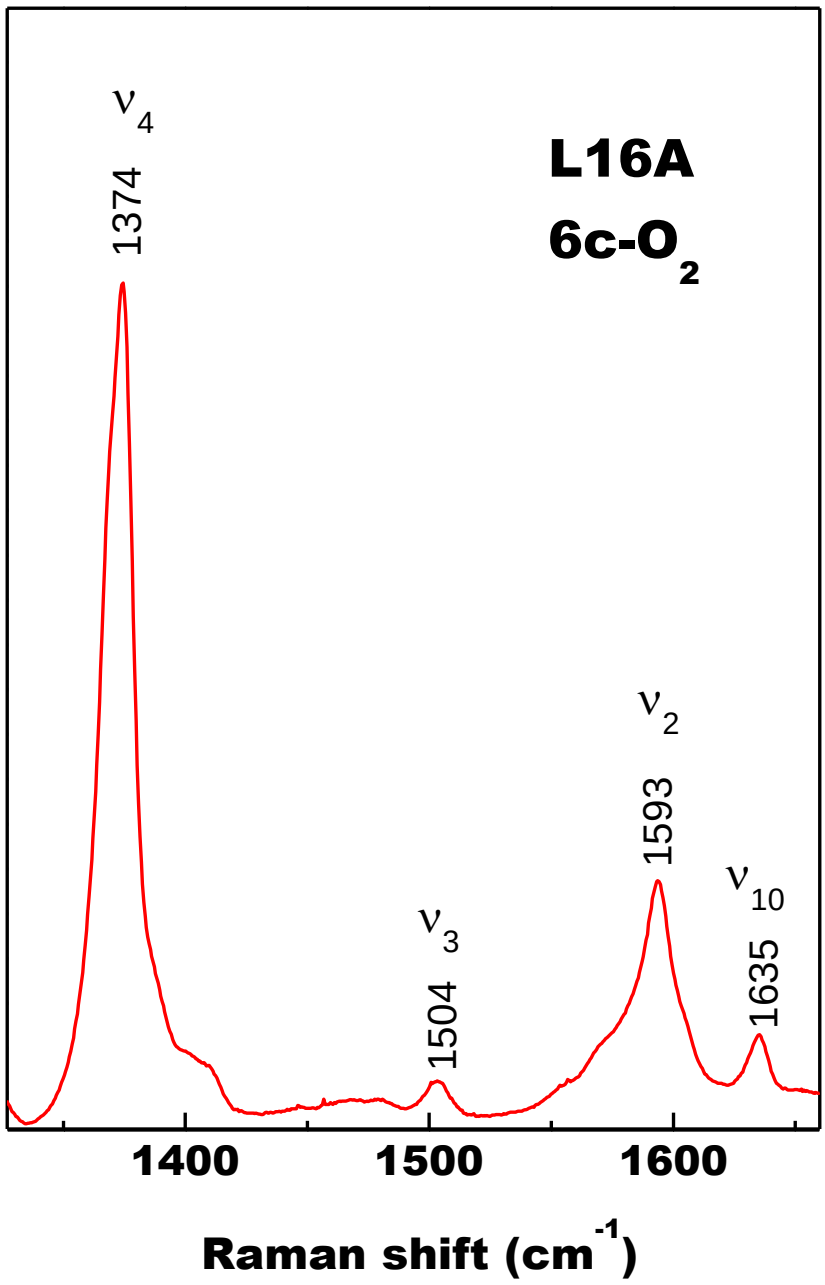

Figure S3. Pseudo-first-order rate constants, k_{obs}, for the reaction of O_2 with Fe^{2+} L16A AXCP as a function of O_2 concentration at 25.0 °C.

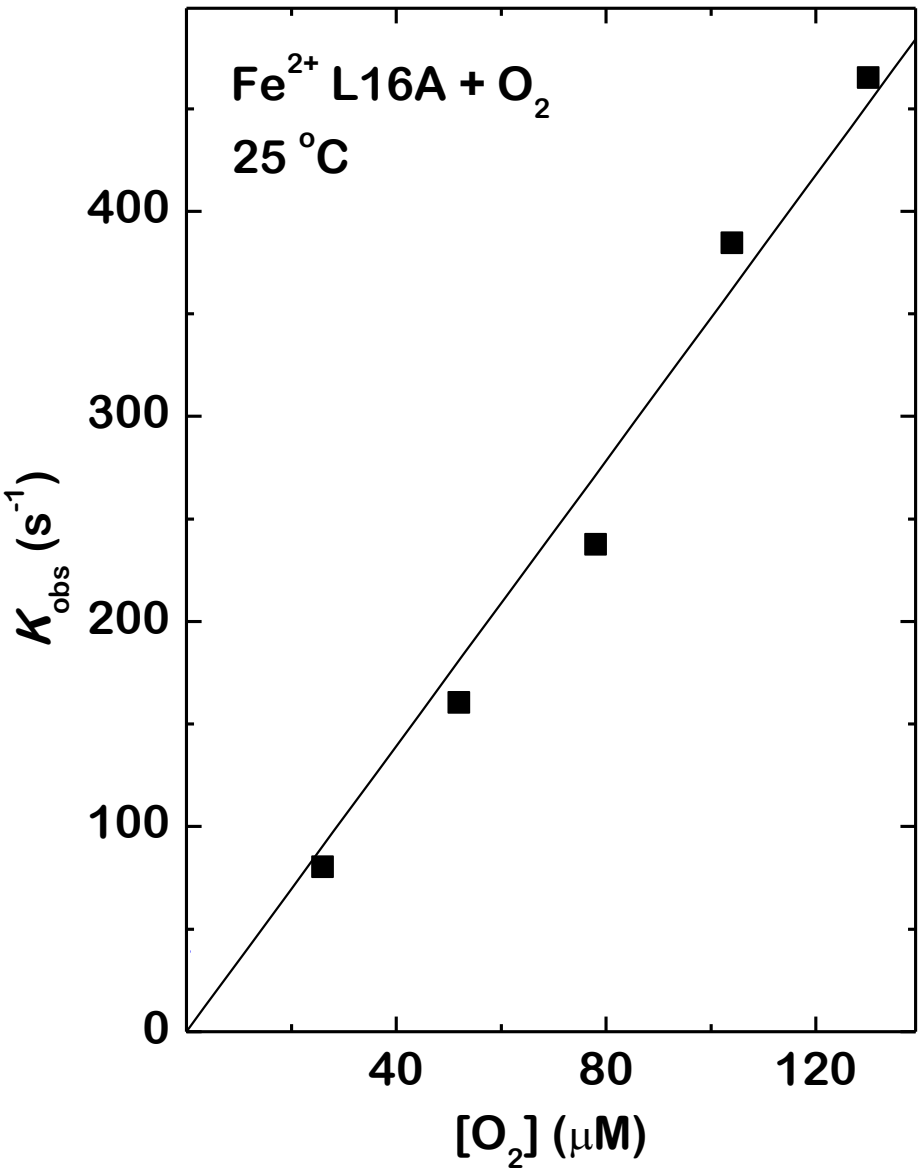

Figure S4. Time trace at 418 nm for the release of O_2 from oxy L16A AXCP in the presence of 5 mM dithionite and 0.5 mM CO at 25.0 °C. Overlaid and mostly obscured is a single-exponential fit.

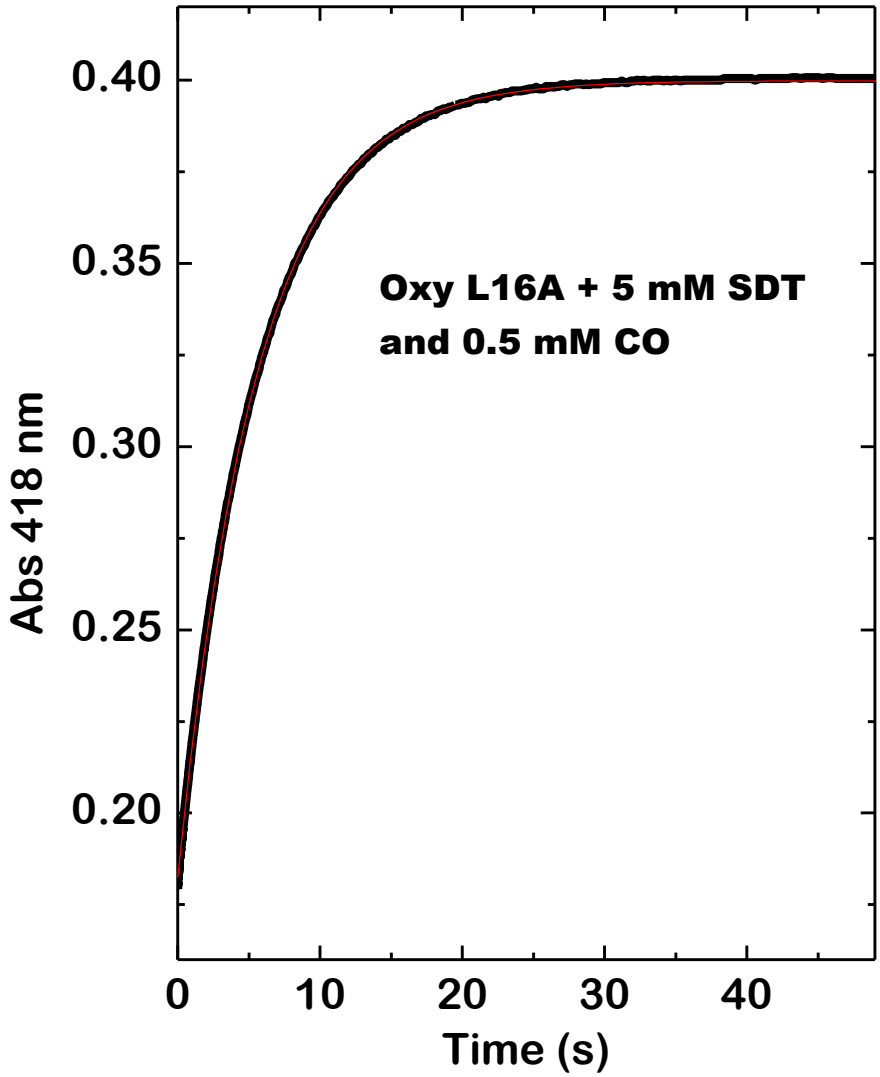

Figure S5. Time-dependent changes in the absorbance spectrum of oxy L16A AXCP at pH 8.9. The spectrum of ferric L16A AXCP at pH 8.9 is shown for comparison.

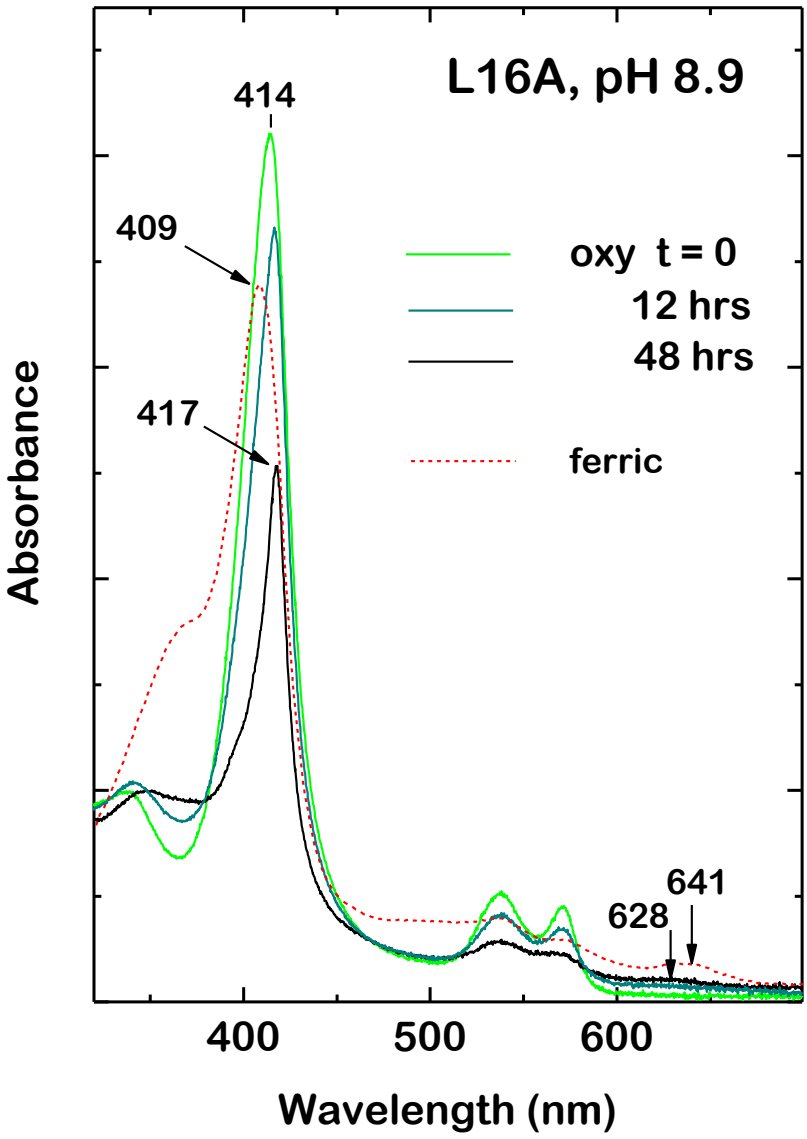

Figure S6. Time-dependent absorbance changes showing the autoxidation of 5c-Fe^{2+} native AXCP (λ_{max} 424 nm) to the 5c-Fe^{3+} state (λ_{max} 406, 640 nm) upon reaction with an air-saturated buffer at pH 8.9, 25 °C. Direct ferrous → ferric conversion (without a detectable oxy complex) is confirmed by the presence of isosbestic points at 325, 414, 455, 528, and 588 nm. The inset shows a reaction time trace at 429 nm (black), overlaid with a 1 exp fit (red).

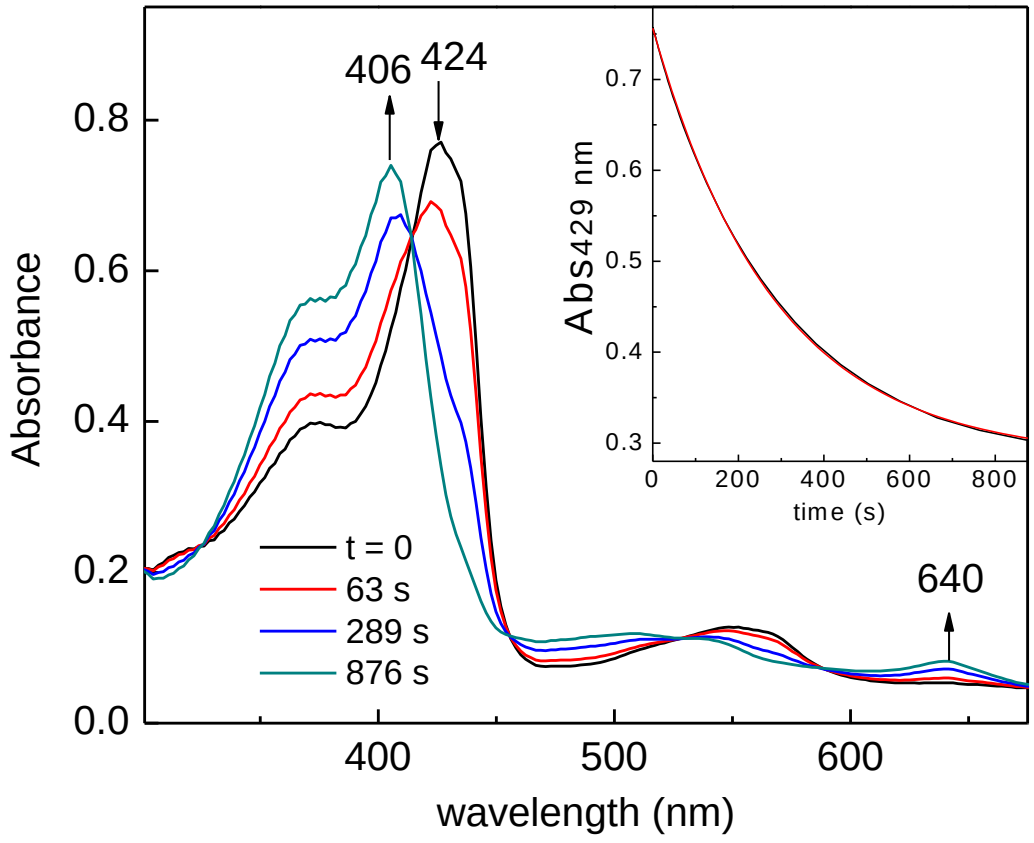

Figure S7. Room-temperature RR spectra of Fe^{2+} L16A AXCP in the high frequency region (413 nm excitation) with the low frequency region (442 nm excitation) shown as an inset. Asterisks denote possible contributions from a trace amount of heme-CO complex. The ν(Fe–His) stretching frequency of L16A AXCP (230 cm^{-1}) is similar to that previously reported for native AXCP (231 cm^{-1})

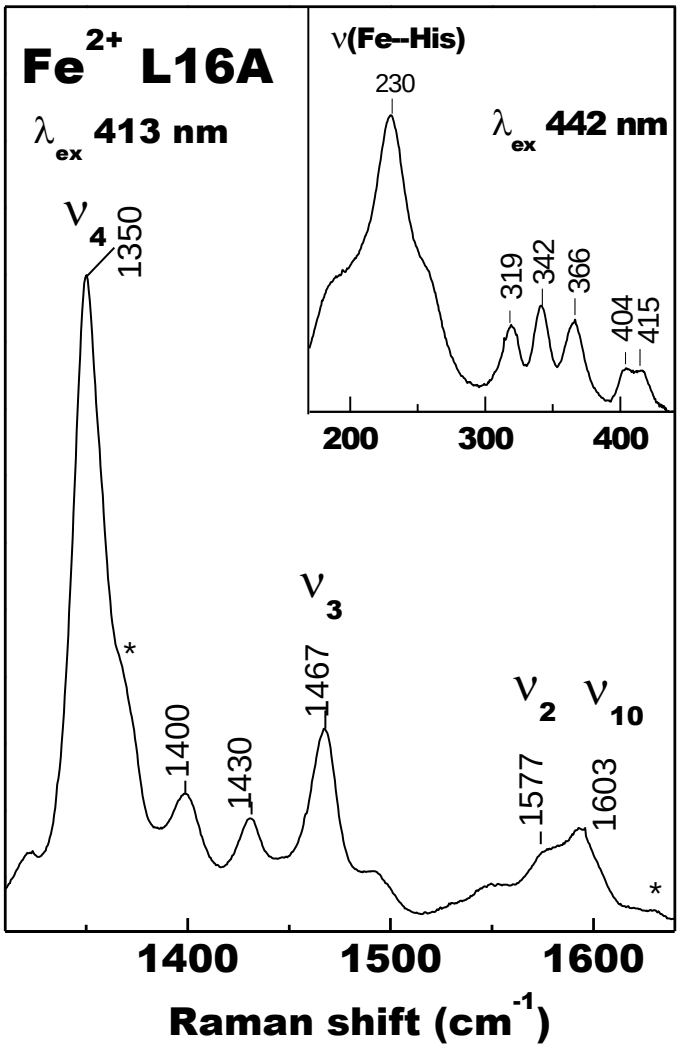

Figure S8 (a) Absorption spectra of ferrous L16A AXCP (solid line) and its NO complex (dotted line). The inset shows a 416-nm time trace for the NO binding reaction in the presence of 42 μM NO, overlaid with a single exponential fit. **(b)** Plot of k_{obs} vs [NO] for NO binding to ferrous L16A AXCP yielding $k_{on}(NO) = 2.9 \times 10^6\ M^{-1}\ s^{-1}$.

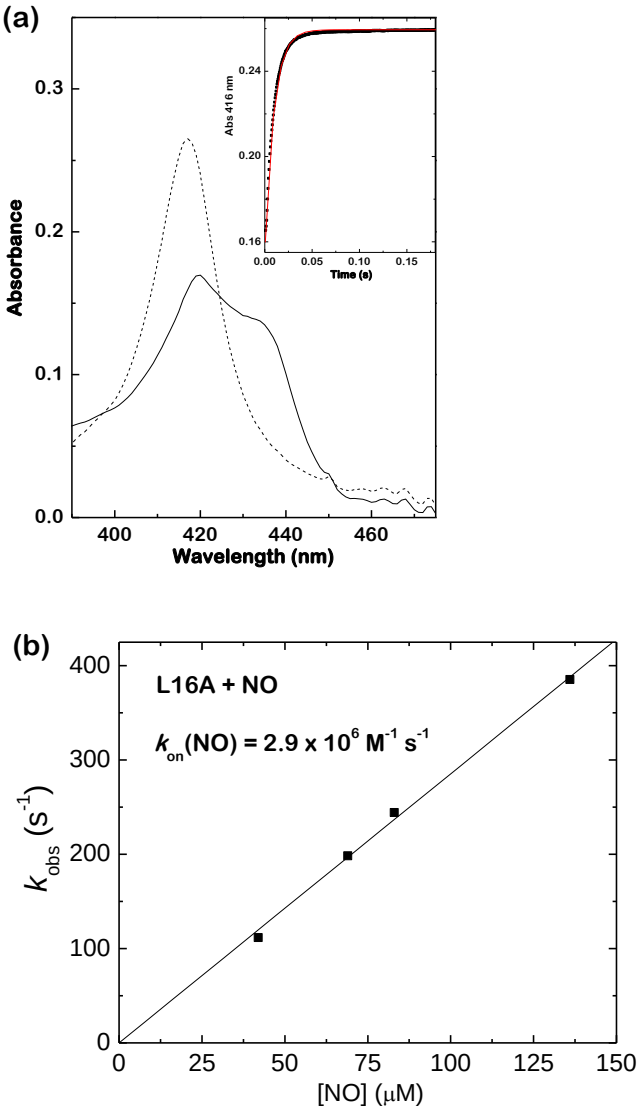

Figure S9 (a) Absorption data showing NO release from L16A AXCP in the presence of 25 mM dithionite and 0.5 mM CO. Heme-NO release is apparent from the conversion of the 6c-NO complex (magenta trace) to the 6c-CO complex (absorption of the pure 6c-CO species shown as a dotted trace). The blue trace shows the reaction after 19 days (estimated ~20% complete). **(b)** 417-nm time trace overlaid with a single exponential fit (red line), with the final absorbance constrained to that predicted for the pure 6c-CO end product. The kinetic fit, yielding $k_{off(NO)}$ = 0.013 day^{-1} (~ 2 × 10^{-7} s^{-1}), has been extended beyond the experimental data to illustrate the predicted reaction time course.

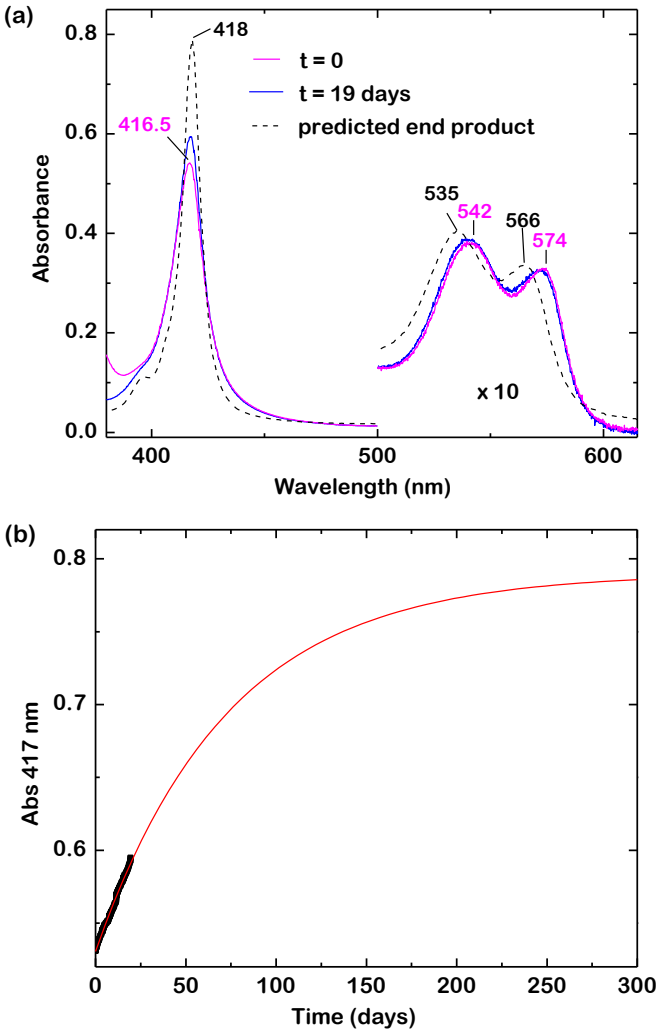

REFERENCES

(1) Antonyuk, S.; Rustage, N.; Petersen, C. A.; Arnst, J. L.; Heyes, D. J.; Sharma, R.; Berry, N.; Scrutton, N. S.; Eady, R. R.; Andrew, C. R.; Hasnain, S. S. *Proc. Natl. Acad. Sci. USA* **2011**, *108,* 15780-15785.

(2) Harris, R. L.; Barbieri, S.; Paraskevopoulos, K.; Murphy, L. M.; Eady, R. R.; Hasnain, S. S.; Sawers, R. G. *J. Mol. Microbiol. Biotechnol*. **2010**, *18*, 102-108.

(3) Olson, J.; Foley, E.; Maillet, D.; Paster, E. *Methods in Molecular Medicine* **2003**, *82*, 65-91.

(4) Andrew, C. R.; Green, E. L.; Lawson, D. M.; Eady, R. R. *Biochemistry* **2001**, *40*, 4115-4122.